

## MODELLING AND OPTIMIZATION OF HYBRID ALUMINIUM COMPOSITE MATERIAL USING RESPONSE SURFACE METHODOLOGY

R.S. Ebhojiaye<sup>1</sup> and E.G. Sadjere<sup>2</sup>

<sup>1</sup>Department of Production Engineering, University of Benin, Benin City, Nigeria.

<sup>2</sup>Department of Mechanical Engineering, University of Benin, Benin City, Nigeria.

### Abstract

*This study was aimed at modelling and optimizing mechanical properties (i.e. wear rate, creep rate, density, tensile strength, hardness and melting temperature) of a composite material fabricated from the combination of 99.85% pure aluminium ingot, periwinkle shell and palm kernel shell particles in a determined mix ratio using the central composite design (CCD) of the response surface methodology (RSM). The results of the mechanical properties obtained for the different compositions of the fabricated specimens were modeled and optimized in this study. Multi-objective numerical optimization was done to ascertain the desirability of the overall model. The obtained optimal blend solution (i.e. predicted values) of the input variables was validated by producing specimens with the optimal solution values and obtaining the mechanical properties (i.e. empirical values). The RSM analysis gave an optimal composition of the aluminium ingot, periwinkle shell and palm kernel shell particles at 97.3% desirability value. A coefficient of determination ( $R^2$ ) value of 0.9997 (i.e. 99.97%) was obtained when the predicted values from RSM was plotted against the empirical values. The  $R^2$  value showed that the model could explain 99.97% of the variance between predicted and empirical values, indicating that there is no significant difference between the predicted values and the empirical values that were obtained.*

**Keywords:** Wear Rate; Creep Rate; Density; Tensile Strength; Hardness; Melting Temperature; Optimal Blend Solution.

### 1.0 Introduction

Today composite material appears to be the material of choice in engineering applications as it has found increasingly wider use in automotive components, sporting goods, aerospace parts, consumer goods, marine and oil industries, offshore structures, piping, electronics, etc. [1,2,3]. Composite materials have the potential of competing with widely used engineering materials like steel and aluminium. Pal et al. [3] reported that 60 to 80% in component weight can be saved when steel part is replaced with composite material and 20 to 50% in component weight when aluminium part is replaced with composite material.

Montgomery [4] described response surface methodology (RSM) as a set of mathematical and statistical techniques which can be used to model and analyze problems in which several variables influence the response of interest and the objective is to optimize this response. The response surface can be mathematically illustrated by wanting for example, to find the levels of temperature ( $x_i$ ) and pressure ( $x_{ii}$ ) that maximize the yield ( $y$ ) of a process. However, the process yield is a function of the levels of temperature and pressure,

$$\text{i.e. } y = f(x_i, x_{ii}) + \epsilon \quad (1)$$

the symbol  $\epsilon$  represents the observed noise or error in the response  $y$ . If the expected response is denoted as,

$$E(y) = f(x_i, x_{ii}) = \eta \quad (2)$$

then the surface which is

$$\eta = f(x_i, x_{ii}) \quad (3)$$

is actually the response surface. Response surface designs are essentially those designs for fitting response surfaces [4].

---

Corresponding Author: Ebhojiaye R.S., Email: Raphael.ebhojiaye@uniben.edu, Tel: +2348028972265

According to Montgomery [4], RSM was first introduced by G.E.P. Box and K.B. Wilson in 1951 as an empirical statistical technique employed for multiple regression analysis of quantitative data obtained from statistically designed experiments. RSM is usually represented graphically as surface plot or contour plot.

Usually, the first stage in RSM is to find a suitable approximation for the true functional relationship between the response and the set of independent variables. A low-order polynomial in some region of the independent variables is commonly used. For a response that is modelled by a linear function of the independent variables, the approximating function is the first-order-model below [4]:

$$y = \beta_0 + \beta_1 x_1 + \beta_2 x_2 + \dots + \beta_k x_k + \epsilon \quad (4)$$

where,  $y$  = response

$\beta_0$  = intercept

$\beta_{1-k}$  = regression coefficients

$x_{1-k}$  = independent variables

$\epsilon$  = error term.

The second-order models are fitted using the central composite design (CCD). The CCD is the most frequently used among the classes of designs for fitting models. Other methods are the Box-Behnken design, equiradial designs, small composite design and hybrid design. The CCD is a very efficient design for fitting second-order model. Two parameters must be specified in the CCD design, these are the distance  $\alpha$  of the axial runs from the design centre and the number of centre points  $n_c$  [4]. According to Montgomery [4], blocking in response surface design is often necessary in order to eliminate nuisance level, which is mostly caused by the sequential assembly from a first-order design to a second order design. Orthogonal blocking in RSM is achieved if it is divided into blocks such that the parameters estimation of the RSM is not really affected by the blocking effects.

## 2.0 Methodology

The materials used in this study included pure aluminium ingot, periwinkle shell particles, palm kernel shell particles and pure magnesium powder. The central composite design (CCD) of the response surface methodology (RSM) was used to perform the design of experiment (DoE). The hybrid composite was formulated and fabricated by stir casting process. In order to aid uniform mix of the reinforcement materials in the matrix, a stir casting rig was used to thoroughly stir the composite in molten state.

Specimens containing these materials at different aggregate levels by % wt. were cast and tested at the laboratory for wear rate, creep rate, density, tensile strength, hardness and melting temperature. The results were recorded as the obtained values for the mechanical properties of the composites composition. RSM was used to optimize the values of the mechanical properties of the prepared composite specimens. Central composite design (CCD) was used in the optimization of process variables with three factors at three levels with 20 runs, including six (6) central points, six (6) axial points and eight (8) factorial points as shown in Table 1. The responses function was partitioned into linear, interactive and quadratic components. Experimental data were fitted to the second-order regression equation.

**Table 1: Summary of Results of all the Mechanical Tests Conducted**

Run	Response 1 Wear Rate (g/s) $10^{-4}$	Response 2 Creep Rate % Elongation/hr	Response 3 Density kg/m <sup>3</sup>	Response 4 Tensile Strength MPa	Response 5 Hardness BHN	Response 6 Melting Temperature °C
1	0.61	14.29	2653.57	94.32	291.08	935
2	0.83	15.79	2645.18	96.62	280.07	930
3	0.67	13.64	2635.74	95.59	282.77	930
4	0.61	16.67	2646.11	94.18	285.49	925
5	0.56	15	2646.91	95.94	291.08	930
6	0.94	15	2648.21	95.64	282.77	935
7	1.67	21.67	2574.06	85.55	121.07	909
8	0.61	58.89	2573.94	93.69	412.54	925
9	1.17	42.94	2637.81	87.71	194.21	880
10	0.67	66.67	2652.77	80.66	138.00	894
11	1.33	11.87	2660.90	80.68	162.69	860
12	1.28	41.78	2643.46	83.07	200.48	880
13	1.78	18.45	2624.24	88.99	138.00	870
14	1.22	13.25	2636.08	86.93	106.86	840
15	0.89	53.37	2661.46	92.36	321.56	868
16	1.39	11.65	2625.46	75.52	324.86	890
17	0.78	18.7	2609.12	74.02	299.75	932
18	1.11	28.7	2657.07	96.53	277.42	899
19	1.06	37.96	2479.17	95.83	299.75	920
20	1.72	22.27	2672.24	88.67	200.48	896

The design and optimization was done using statistical design software. For this study, Design Expert 7.01 was employed. The model standard errors were computed to assess the suitability of RSM, the goodness of fit (GOF) statistics was used to validate the model adequacy in terms of the R-squared, adjusted R-squared and adequate precision values of and adjusted. Analysis of variance (ANOVA) was employed to determine the significance of the models. The optimal equations in terms of the actual factors were obtained for the six responses. The 3-D surface plot was used to study the effects of the combined variables on each response. Multi-objective optimization was done to ascertain the desirability of the overall model. The desirability bar graph was used to show the accuracies with which the model predicted the six responses. Contour plots were used to show the predicted values. The model validity was confirmed by obtaining the R-squared value from the plot of the optimised solution against the empirical values.

**3.0 Result and Discussion**

The results of the RSM analysis are presented and discussed.

**3.1 The model Standard Error Analysis**

The computed standard errors for the selected responses which were used to assess the suitability of response surface methodology are presented in Figure 1.

Term	StdErr**	VIF	R-Squared	0.5 Std. Dev.	1 Std. Dev.	2 Std. Dev.
A	0.27	1.00	0.0000	13.3 %	38.6 %	91.4 %
B	0.27	1.00	0.0000	13.3 %	38.6 %	91.4 %
C	0.27	1.00	0.0000	13.3 %	38.6 %	91.4 %
AB	0.35	1.00	0.0000	9.8 %	24.9 %	72.2 %
AC	0.35	1.00	0.0000	9.8 %	24.9 %	72.2 %
BC	0.35	1.00	0.0000	9.8 %	24.9 %	72.2 %
A <sup>2</sup>	0.26	1.02	0.0179	40.4 %	92.7 %	99.9 %
B <sup>2</sup>	0.26	1.02	0.0179	40.4 %	92.7 %	99.9 %
C <sup>2</sup>	0.26	1.02	0.0179	40.4 %	92.7 %	99.9 %

\*\*Basis Std. Dev. = 1.0

**Figure 1: Result of Computed Standard Errors of the Model**

Figure 1 shows that the model has a low standard error ranging from 0.27 for the individual terms, 0.35 for the combined effects and 0.26 for the quadratic terms. The error values were also observed to be less than the model basic standard deviation of 1.0 which suggested that the response surface methodology was ideal for the optimization process. Also the variance inflation factor (VIF) of approximately 1.0 was obtained which is good since ideal VIF is 1.0. The Ri-squared values were observed to be between 0.0000 and 0.0179 which is good. High Ri-squared (above 0.1) means that design terms are correlated with each other, possibly leading to poor models.

**3.2 The Goodness of Fit Analysis**

To validate the adequacy of the model based on its ability to satisfy the set objectives the goodness of fit (GOF) statistical analysis was done as shown in Figures 2 to 7.

Std. Dev.	R-Squared
0.11	0.9401
Mean	Adj R-Squared
1.04	0.9014
C.V. %	Pred R-Squared
10.83	0.5854
PRESS	Adj Precision
1.00	14.272

**Figure 2: GOF of the Wear Rate**

Std. Dev.	R-Squared
7.68	0.9248
Mean	Adj R-Squared
36.29	0.6572
C.V. %	Pred R-Squared
21.16	0.4271
PRESS	Adj Precision
4485.17	9.885

**Figure 3: GOF of the Creep Rate**

Std. Dev.	R-Squared
43.54	0.9011
Mean	Adj R-Squared
2628.81	0.8121
C.V. %	Pred R-Squared
1.66	0.2342
PRESS	Adj Precision
1.525E+005	12.546

**Figure 4: GOF of the Density**

Std. Dev.	R-Squared
2.30	0.9529
Mean	Adj R-Squared
88.04	0.9106
C.V. %	Pred R-Squared
2.59	0.6229
PRESS	Adj Precision
425.50	15.118

**Figure 5: GOF of the Tensile Strength**

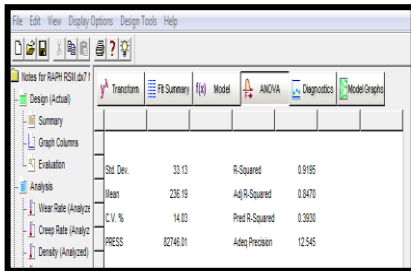


Figure 6: GOF of the Hardness

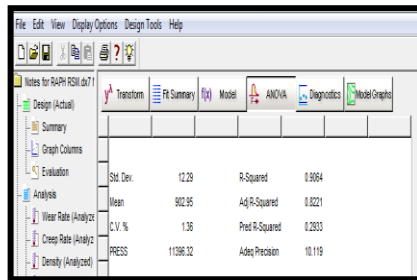


Figure 7: GOF of the Melting Temperature

Coefficient of determination (R-Squared) values of 0.9481, 0.9248, 0.9011, 0.9529, 0.9195 and 0.9064 as shown in Figures 2 to 7 respectively revealed the extent to which the model was able to predict the responses. According to Montgomery [4], the closer the  $R^2$  value is to 1 (i.e. unity) the better the ability of the model to predict the response. Adjusted (R-Squared) values of 0.9014, 0.8572, 0.8121, 0.9106, 0.8470 and 0.8221 as shown in Figures 3 to 8 respectively, gave model reliability of 90.14%, 85.72%, 81.21%, 91.06%, 84.70% and 82.21% respectively. The coefficient of variation (CV) obtained were 10.8%, 21.16%, 1.66%, 2.59%, 14.03% and 1.36% respectively. These relatively low values of CV obtained showed high precision and reliability of the model [5]. Adequate precision values of 14.272, 9.895, 12.546, 15.118, 12.545 and 10.119 showed an adequate signal that is desirable. Therefore, this model can be used to navigate the design space and obtain the set objectives. Adequate precision measures the signal to noise ratio. A ratio greater than 4 is desirable [6].

3.3 One Way Analysis of Variance

A one way analysis of variance (ANOVA) was done to check for the model significance for each response variable. The results are shown in Figures 8 to 13.

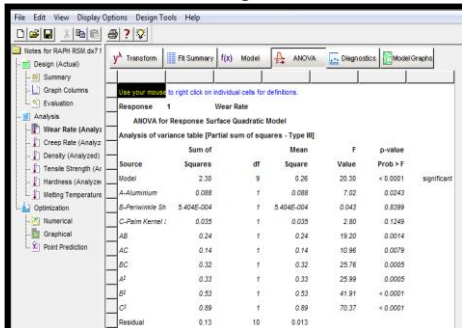


Figure 8: ANOVA Table the Wear Rate

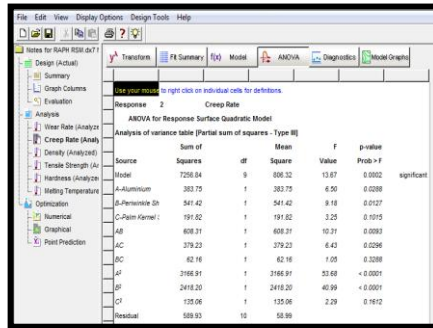


Figure 9: ANOVA Table the Creep Rate

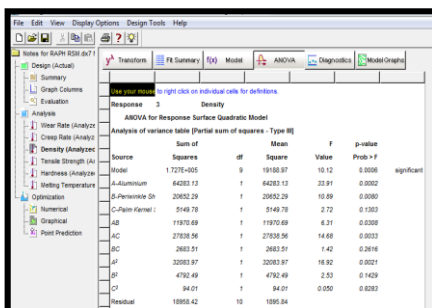


Figure 10: ANOVA Table for the Density

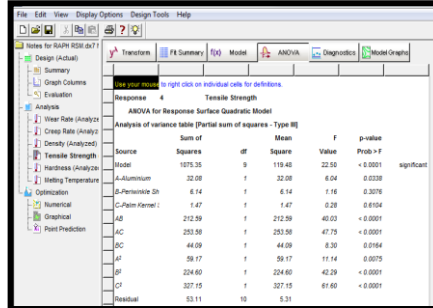


Figure 11: ANOVA Table for the Tensile Strength

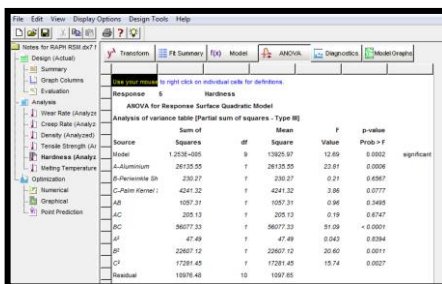


Figure 12: ANOVA Table for the Hardness

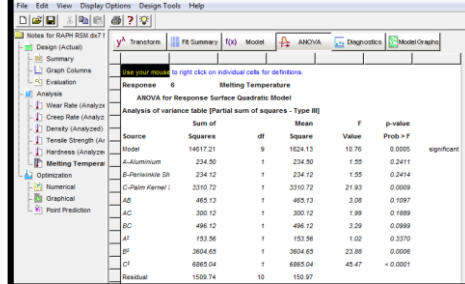


Figure 13: ANOVA Table for Melting Temperature

From the one way ANOVA analysis in Figure 8, the significant model has an F-value (or test statistics value) of 20.30 and p-value (significant level) of 0.0001. This implies that there is only a 0.01% chance that a "Model F-Value" this large could occur due to noise. In this case, the significant models terms included: A, AB, AC, BC,  $A^2$ ,  $B^2$ ,  $C^2$  because, Values of "Prob > F" less than 0.0500 and greater than 0.1000 indicate significant and insignificant models respectively [7,8]. The respective significant terms had p-values less than 0.05 and are therefore significant models.

Figure 9 shows the Model F-value of 13.67 with computed p-value of 0.0002. There is only a 0.02% chance that a "Model F-Value" this large could occur due to noise. In this case A, B, AB, AC,  $A^2$ ,  $B^2$  are significant model terms.

Figure 10 shows the Model F-value of 10.12 with computed p-value of 0.0006. There is only a 0.06% chance that a "Model F-Value" this large could occur due to noise. In this case A, B, AB, AC,  $A^2$  are significant model terms.

Figure 11 shows the Model F-value of 22.50 with a computed p-value of 0.0001. There is only a 0.01% chance that a "Model F-Value" this large could occur due to noise. In this case A, AB, AC, BC,  $A^2$ ,  $B^2$ ,  $C^2$  are significant model terms.

Figure 12 shows the Model F-value of 12.69 with computed p-value of 0.0002. There is only a 0.02% chance that a "Model F-Value" this large could occur due to noise. In this case A, BC,  $B^2$ ,  $C^2$  are significant model terms.

Figure 13 shows the Model F-value of 10.76 with computed p-value of 0.0005. There is only a 0.05% chance that a "Model F-Value" this large could occur due to noise. In this case C,  $B^2$ ,  $C^2$  are significant model terms.

### 3.4 Optimal Equations of the Models

The optimal equations which shows the individual effects and combined interactions of the selected variables against the measured responses are presented based on the actual factors as shown in Figures 14 to 19.

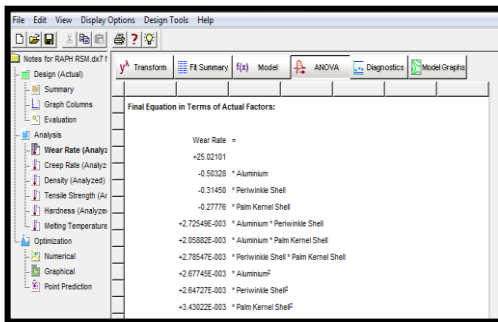


Figure 14: Optimal Equation for Wear Rate

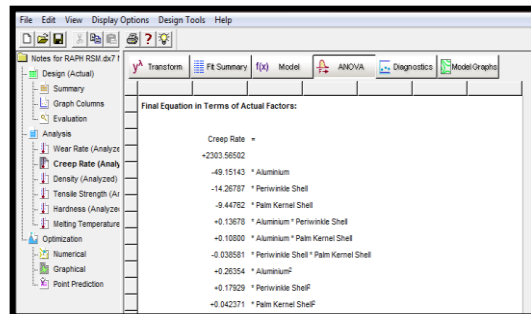


Figure 15: Optimal Equation for Creep Rate

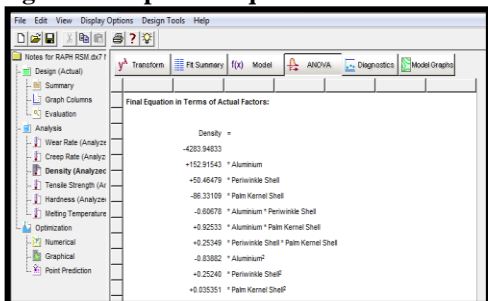


Figure 16: Optimal Equation for Density

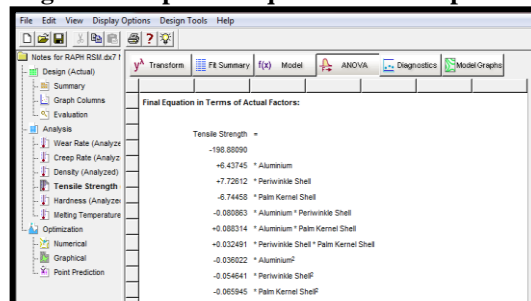


Figure 17: Optimal Equation for Tensile Strength

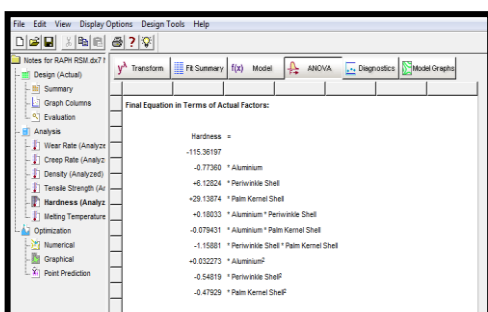


Figure 18: Optimal Equation for Hardness

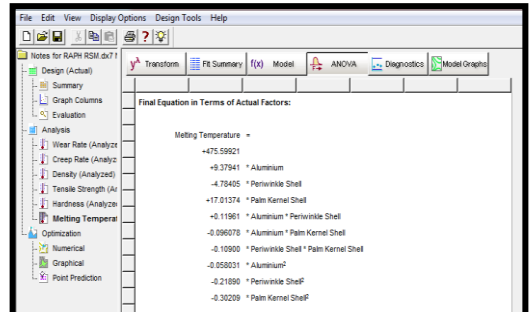


Figure 19: Optimal Equation for Melting Temp.

The optimal equations of the actual factors for the six responses by the second order polynomial equation are represented as:  $y = \beta_0 + \beta_1A + \beta_2B + \beta_3C + \beta_4AB + \beta_5AC + \beta_6BC + \beta_7A^2 + \beta_8B^2 + \beta_9C^2(5)$

where,  $y$  = response

$\beta$ 's = regression coefficients

$A$  = aluminium

$B$  = periwinkle shell

$C$  = palm kernel shell

$AB$  = aluminium and periwinkle shell

$AC$  = aluminium and palmkernel shell

$BC$  = periwinkle shell and pal kernel shell

From Figures 14 to 19, the optimal equations for the actual factors for all the responses are:

1. Wear Rate ( $y_1$ ):

$$y_1 = 25.021 - 0.503A - 0.315B - 0.278C + 0.00273AB + 0.00205AC + 0.00279BC + 0.00268 A^2 + 0.00265B^2 + 0.00343 C^2 \tag{6}$$

2. Creep Rate ( $y_2$ ):

$$y_2 = 2303.565 - 49.151A - 14.268B - 9.448C + 0.137AB + 0.108AC - 0.039BC + 0.263A^2 + 0.179B^2 + 0.042 C^2 \tag{7}$$

3. Density ( $y_3$ ):

$$y_3 = -4283.948 + 152.915A + 50.465B - 86.331C - 0.607AB + 0.925AC + 0.253BC - 0.839A^2 + 0.252B^2 + 0.035C^2 \tag{8}$$

4. Tensile Strength ( $y_4$ ):

$$y_4 = -198.881 + 6.437A + 7.726B - 6.745C - 0.081AB + 0.088AC + 0.032BC - 0.036A^2 - 0.0545B^2 + 0.0666C^2 \tag{9}$$

5. Hardness ( $y_5$ ):

$$y_5 = -115.362 - 0.774A + 6.128B + 29.139C - 0.180AB - 0.079AC - 1.159BC + 0.032A^2 - 0.548B^2 - 0.479C^2 \tag{10}$$

6. Melting Temperature ( $y_6$ ):

$$y_6 = 475.599 + 9.379A - 4.784B + 17.014C + 0.119AB - 0.096AC - 0.109BC - 0.058A^2 - 0.219B^2 + 0.302C^2 \tag{11}$$

### 3.6 Multi-objective Numerical Optimization of the Model

Multi-objective optimization was performed to ascertain the desirability of the overall model. In the numerical optimization phase, we requested design expert to minimize the wear rate, creep rate and density while maximizing the tensile strength, hardness and melting temperature in order to determine the optimum values of aluminium, periwinkle shell and palm kernel shell. The interfaces of the numerical optimization are shown in Figures 20 to 25.

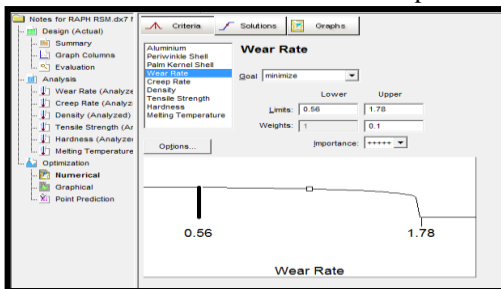


Figure 20: Optimization Model for Wear Rate

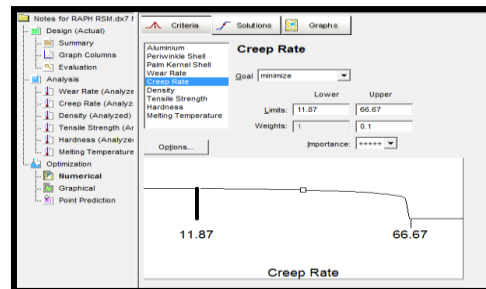


Figure 21: Optimization Model for Creep Rate

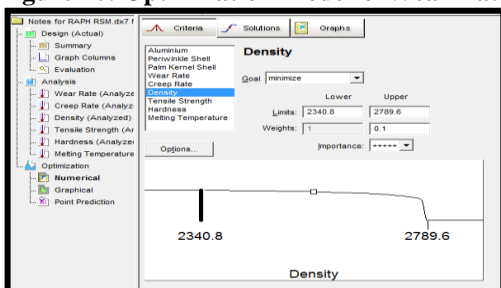


Figure 22: Optimization Model for Density

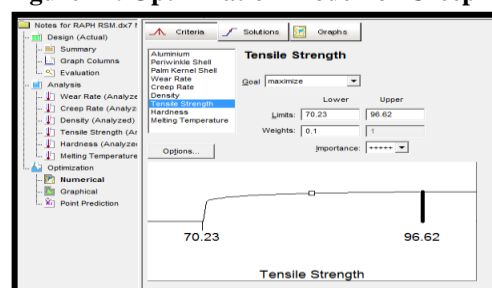


Figure 23: Optimization Model for Tensile Strength



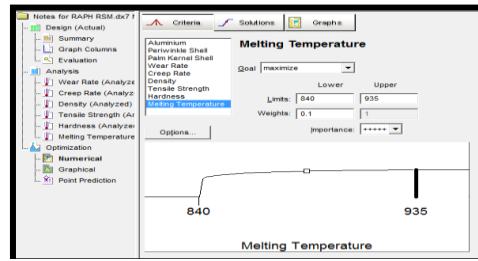
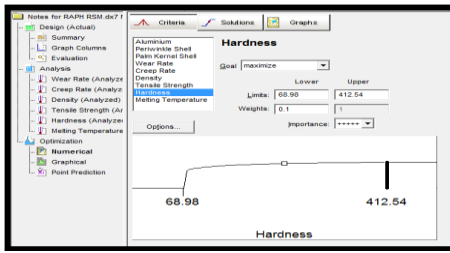


Figure 24: Optimization Model for Hardness

Figure 25: Optimization Model for Melting Temp.

The constraint set for the numerical optimization algorithm is shown in Figure 26. While Figure 27 shows the three (3) optimal solutions that was given by the numerical optimization process.

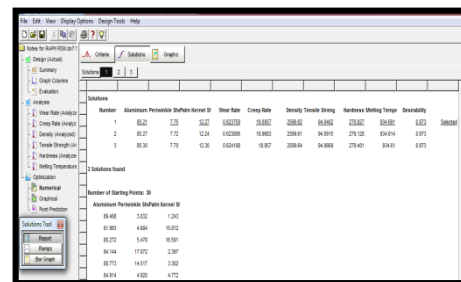
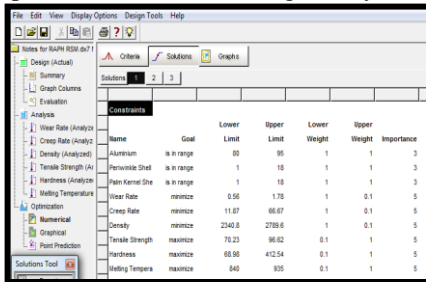


Figure 26: Constraints for Numerical Optimization of Selected Responses

Figure 27: Optimal Solutions of Numerical Optimization Model

From the results in Figure 27, the optimum mix ratio of the input variables will produce an engineering composite material with optimum values for each of the responses at a desirability value of 97.3%.

3.7 Analysis of Model Prediction Accuracy

The desirability bar graph which shows the accuracy with which the model was able to predict the values of the selected input variables and the corresponding responses as shown in Figure 28 was used to check the model prediction accuracy.

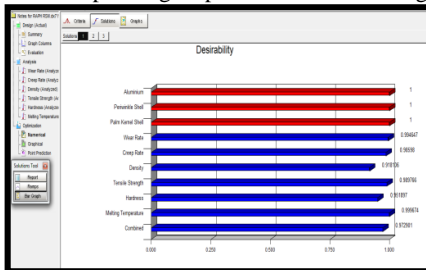


Figure 28: Prediction Accuracy of Numerical Optimization

Figure 28 shows that the model developed based on response surface methodology and optimized using numerical optimization method, predicted the wear rate with an accuracy of 99.46%, creep rate with an accuracy of 98.60%, density with an accuracy of 91.81%, tensile strength with an accuracy of 98.98%, hardness with an accuracy of 95.97% and melting temperature with an accuracy of 99.97%.

3.8 Validation of Optimal Solution of the RSM Analysis

The optimal blend solution of the input variables of aluminium ingot, PS and PKS that was obtained from the RSM analysis, was validated by producing specimens with the optimal blend solution values. The specimens were tested for creep rate; wear rate; density; tensile test; hardness; and melting temperature. Figure 29 shows the experimental (empirical) values and optimal solution values obtained from the RSM analysis (i.e. predicted).

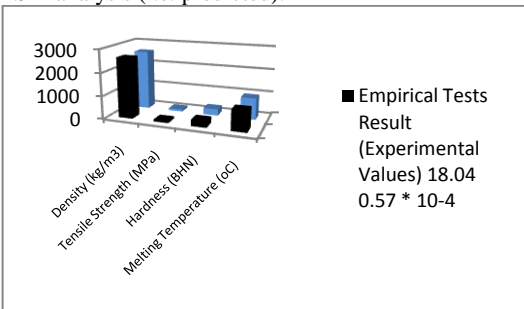
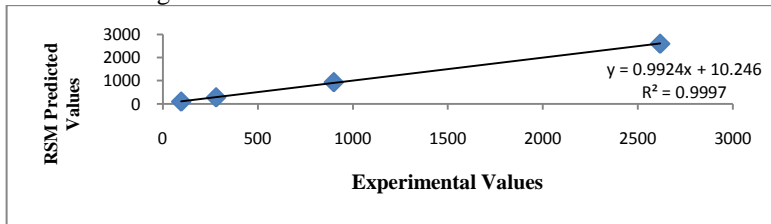


Figure 29: Empirical Results against RSM Results of Optimal Blend Solution

The values shown in Figure 29 obtained for the optimal solution of the RSM analysis (i.e. predicted values) and that obtained from the empirical tests (i.e. experimental values) for the six responses (i.e creep rate, wear rate, density, tensile strength, hardness and melting temperature) were tested for variability by determining the coefficient of determination (i.e.  $R^2$ ) value as shown in Figure 30.



**Figure 30: Plot of RSM Predicted Values against Experimental Values**

A coefficient of determination ( $R^2$ ) value of 0.9997 (i.e. 99.97%) was obtained when the predicted values from RSM was plotted against experimental values obtained as shown in Figure 30. The  $R^2$  value showed that the model could explain 99.97% of the variance between predicted and experimental values. Therefore, there is no significant difference between predicted values and experimental values obtained.

#### 4. Conclusion

The CCD method of the RSM was used to successfully optimize some sets of experimental values that were obtained as mechanical properties of locally fabricated hybrid composite material made of different mix compositions of pure aluminium ingot, periwinkle shell (PS) and palm kernel shell. From the study the following conclusions were drawn:

- (i) That an optimum composition ratio of 80.98 wt. % aluminiumingot,  $OPT_1$  wt. % PS and  $OPT_2$  wt. % PKSoF the composite materials were obtained.
- (ii) The obtained optimum composition produced the following mechanical properties: wear rate of  $0.623758 * 10^{-4}$  g/s; creep rate of 19.0857% elongation/hr; density of  $2598.62 \text{kg/m}^3$ ; tensile strength of 94.0402MPa; hardness of 278.827BHN; and melting temperature of 934.691°C.
- (iii) That the reinforcement materials (i.e. PS and PKS) substantially influenced the mechanical properties of the pure aluminium ingot used as the matrix.
- (iv) That there was no significant difference between predicted values and experimental values obtained which validated the optimization result obtained.

#### 5. References

- [1] Schwartz, M. (1984) "Composite Material Handbook". McGraw-Hill, New York.
- [2] Kalpakjian, S. and Schmid, S.R. (2001) "Manufacturing Engineering and Technology". 4th Edition, Pearson Education, Inc., USA.
- [3] Pal, H., Jit, N., Tyagi, A.K. and Sidhu, S. (2011) "Metal Casting – A general Review". *Advances in Applied Science Research*, Vol. 2, No. 5, pp. 360 – 371.
- [4] Montgomery, D.C. (2001) "Design and Analysis of Experiments". 5th Edition, New York, John Wiley and Sons, Inc.
- [5] Hou, X.J. and Chen, W. (2008) "Optimization of Extraction Process of Crude Polysaccharides from Wild Edible Bachu Mushroom by Response Surface Methodology". *Carbohydrate Polymers*, Vol. 72, pp. 67 – 74.
- [6] Qi, B., Chen, X., Shen, F. and Wan, Y. (2009) "Optimization of Enzymatic Hydrolysis of Wheat Straw Preheated by Alkaline Peroxide using Response Surface Methodology." *Industrial and Engineering Chemistry Research*, Vol. 48, pp. 7346 – 7353.
- [7] Daniel, W.W. (2002) "In: Biostatistics". 7th Edition. New York: John Wiley and Sons, Inc; Hypothesis testing; pp. 204 – 294.
- [8] Banerjee, A., Chitnis, U.B., Jadhav, S.L., Bhawalkar, J.S. and Chaudhury, S. (2009) "Hypothesis Testing, Type I and Type II Errors". *Industrial Psychiatry Journal*, Vol. 18 (2), pp. 127 – 131.